ISSN 0018-1439, High Energy Chemistry, 2015, Vol. 49, No. 2, pp. 117–121. © Pleiades Publishing, Ltd., 2015.
Original Russian Text © A.E. Galashev, A.A. Galasheva, 2015, published in Khimiya Vysokikh Energii, 2015, Vol. 49, No. 2, pp. 135–140.

NANOSTRUCTURED SYSTEMS AND MATERIALS

Computer Simulation of Cluster Bombardment of a Lead Film on Graphene

A. E. Galashev and A. A. Galasheva

Institute of Industrial Ecology, Ural Division, Russian Academy of Sciences, ul. S. Kovalevskoi 20, Yekaterinburg, 620990 Russia

e-mail: galashev@ecko.uran.ru

Received October 14, 2014; in final form, October 27, 2014

Abstract—The problem of removal of a lead film from partially hydrogenated imperfect graphene by bombarding the target with a beam of Xe_{13} clusters having energies of 5–30 eV and an incident angle of 0° has been solved using the molecular dynamics method. Graphene is completely cleaned of lead at cluster energies of 10 and 15 eV. At higher beam energies, the lead can percolate through divacancies to the back side of graphene or, by virtue of plastic deformation, adhere to the front side. The separation of lead from the graphene film follows the cluster mechanism. The metal film torn off the graphene and acquired the cluster form has the lowest value of the horizontal mobility of the atoms among all of the systems under consideration and quite low values of vertical mobility. The separation of the lead film from the graphene can also result in a significant decrease in the value of certain components of the metal-film stress tensor and an increase in graphene roughness.

DOI: 10.1134/S001814391502006X

Lead is a toxic metal and constitutes an environmental hazard, especially, in atomized form. Use of graphene oxide as a filter material dramatically increases the efficiency of removal of the heavy metals Cu and Pb from an aqueous solution [1]. Trace quantities of heavy metals in water and air can be removed using graphene membrane filters. But this brings up another point: the filters need to be cleaned of the metal deposit. Since the graphene used for membranes has defects, such as the Stone–Wales defects [2], and mono- and polyvacancies, the bonding of the deposited metal to graphene can be significant. A method for graphene cleaning of the metal should be, on one hand, efficient to entirely remove the deposit and, on the other hand, fairly practicable not to damage graphene, thereby providing its multiple reuse.

Bombardment with the cluster "projectile" is milder in comparison with ion bombardment [3], since the cluster projectile cannot penetrate into the target as deep as the atomic analogue does. Simulation of the bombardment of Ag{111} surface with 15-keV C_{60} showed the highest yields of atoms of the target at normal incidence. For heavy targets, the projectiles with an angle of incidence other than normal are prone to easier backscattering into a vacuum. In this case, the effective amount of projectile energy and, hence, the total yield of ejection are lower. Lead has a low energy of adhesion to perfect graphene (0.2 eV) [4]; however, the binding energy of Pb atoms with graphene at the divacancy interface is quite significant (3.4 eV) [5].

The aim of this work was to find an approach to the removal of a lead film from graphene without destroying the latter. Therefore, the energies of the cluster beams were taken to be much smaller than the beam energies used in the experiments, the main objective of which had been sputtering of the bombarded material.

COMPUTER SIMULATION PROCEDURE

Interatomic interactions in graphene were defined by a modified many-body Tersoff potential [6]. The covalent bonding distance was increased to 0.23 nm, and additional weak attraction at $r > 0.23$ nm defined by the Lennard-Jones (LJ) potential with the parameters as given in [7] was included. To eliminate the resulting torque at each lattice site of a graphene sheet, the rotational component of the force generated by the atoms of adjacent sites was excluded. An analytical form of the local rotational interaction potential is given in [7].

Atomic interactions in the lead film were simulated using the Sutton–Chen many-body potential [8]. Lead–carbon and xenon–xenon interactions were defined by the LD potential [9–11]. The interaction between Xe atoms and target (Pb and C) atoms was determined by the purely repulsive ZBL potential [12]

$$\Phi = Z_i Z_j \frac{e^2}{r}\left\{0.1818\exp\left(-3.2\frac{r}{a}\right) + 0.5099\exp\left(-0.9423\frac{r}{a}\right) + 0.2802\exp\left(-0.4029\frac{r}{a}\right) + 0.02817\exp\left(-0.2016\frac{r}{a}\right)\right\}, \quad (1)$$

where Z_i and Z_j are the atomic numbers of the i th and j th atoms, respectively; e is the unit electric charge; r is the distance between the atoms; and a is the parameter defined by the expression:

$$a = 0.8854a_0\left(Z_i^{0.23} + Z_j^{0.23}\right)^{-1}. \quad (2)$$

Here, a_0 is the Bohr radius. We neglect the weak attraction between Xe and Pb atoms on one hand and Xe and C atoms on the other hand, since the primary focus of this study is energy and momentum transfer, rather than chemical bonding [13].

Defects substantially enhance the adhesion of metals to graphene. The most common defects in graphene are divacancies. The graphene sheet used for lead deposition had four divacancies having a nearly even distribution over its surface. To strengthen the edges and borders of the divacancies, hydrogenation was employed. The H groups formed at the edges and in the lattice sites closest to the center of the divacancies were modeled using the single-atom scheme [14]. The C–CH and CH–CH interactions were represented as given by the LJ potential [14]. The partial functionalization of graphene by attaching hydrogen atoms to the edges stabilizes the structure, causing neither increase in the interatomic distances nor creation of roughness over the entire surface.

The lead film on graphene was formed in a separate molecular dynamics (MD) calculation in two steps. In the first step, Pb atoms were placed over the centers of noncontiguous graphene cells so that the distance between Pb and C atoms would be equal to the distance of 2.33 Å calculated using the density functional theory [5]. On this loose lead film consisting of 49 Pb atoms, another 51 Pb atoms were randomly deposited. Then, the system composed of 100 Pb atoms and 406 C atoms was equilibrated at $T = 300$ K in the MD calculation with a duration of 1 million time steps ($\Delta t = 0.2$ fs). The numerical solution of the equations of motion was performed by the fourth-order Runge–Kutta method. The target obtained in this way was then bombarded with icosahedral Xe_{13} clusters. Five starting points for placing the Xe_{13} cluster centers were uniformly spaced apart in a line parallel to the *oy* axis ("chair" direction). This line was almost over the left edge of graphene, with a shift from the edge to the right by σ_{LJ}^{Xe} (σ_{LJ}^{Xe} is the LJ parameter for Xe), at a height of 1.5 nm. The interval of $L_x - 2\sigma_{LJ}^{Xe}$, where L_x is the length of the graphene sheet in the direction of the *ox* axis ("zigzag" direction), was divided into five equal segments with a length L_i. At the beginning of each subsequent cycle of cluster impacts, the line of starting points of Xe_{13} clusters horizontally moved forward to a distance L_i. As a result, the film surface was covered with 25 evenly spaced points, at which cluster impacts were aimed. Each series consisted of 5 cycles or 25 impacts. At the starting point, all of the Xe_{13} cluster atoms received the same downward vertical velocity. Clusters were allowed to shoot in turn to the target. The lifetime of each cluster was limited to 8 ps. After this time, the Xe atoms of the destroyed cluster were excluded from consideration and a new Xe_{13} cluster started moving from another starting point. Bombardment at five different values of cluster energy of 5, 10, 15, 20, and 30 eV was performed using an incidence angle of $\theta = 0°$. The heat released in the system (in both the metal film and graphene) as a result of bombardment was partly dissipated by ejected Pb and Xe atoms and withdrawn using the Berendsen thermostat [15] included in the model.

The total diffusion coefficient of atoms was calculated as

$$D = D_{xy} + D_z = \frac{1}{2\Gamma\tau}\left\langle\left[\Delta\mathbf{r}(t)\right]^2\right\rangle_n, \quad (3)$$

where $\Gamma = 3$ is the dimensionality of space. By $\langle\ldots\rangle$, averaging over n is denoted, where n is the number of time intervals for determination of $\left\langle\left[\Delta\mathbf{r}(t)\right]^2\right\rangle$.

The stress at the location of the i th atom of the metal film is defined by [8]

$$\sigma_{\alpha\beta}(i) = \frac{\varepsilon}{2a^2\Omega_i}\sum_{j\neq i}^{k}\left[-q\left(a/r_{ij}\right)^{q+2} + cs\left(1/\sqrt{\rho_i} + 1/\sqrt{\rho_j}\right)\left(a/r_{ij}\right)^{s+2}\right]r_{ij}^{\alpha}r_{ij}^{\beta}, \quad (4)$$

where ε is the parameter with the dimension of energy; c is a dimensionless parameter; a is the parameter with the dimensions of length, which is usually chosen equal to the lattice constant; q and s are positive integers, wherein $q > s$; and Ω_i, the volume belonging to an individual atom, can be associated with the volume of the Voronoi polyhedron related to the ith atom.

The surface roughness (or arithmetic average roughness height) was calculated according to [16] as

$$R_a = \frac{1}{N}\sum_{i=1}^{N}|z_i - \overline{z}|, \quad (5)$$

where N is the number of sites (atoms) on the graphene surface, z_i is the level of the ith atom, and $\overline{z}$ is the level of the graphene surface, with the values of z_i and $\overline{z}$ being determined at the same point of time.

The obtained value for the total energy of free single-sheet graphene at 300 K is –7.02 eV, which agrees

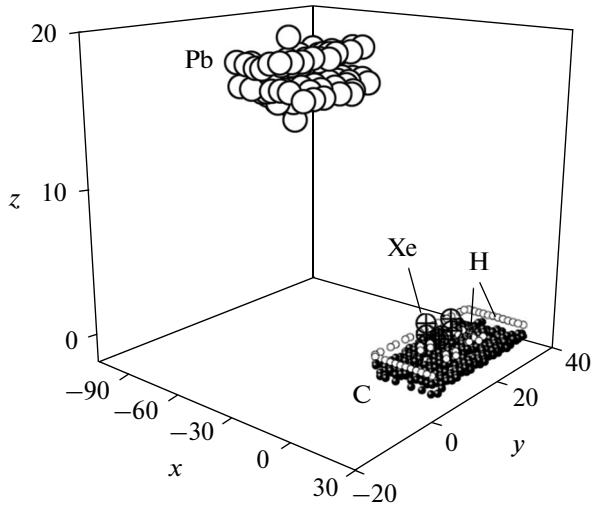

Fig. 1. Configuration of the "Pb film on graphene" target subjected to bombardment with 10-eV Xe_{13} clusters after 125 cluster impacts. The atomic coordinates are given in angstroms.

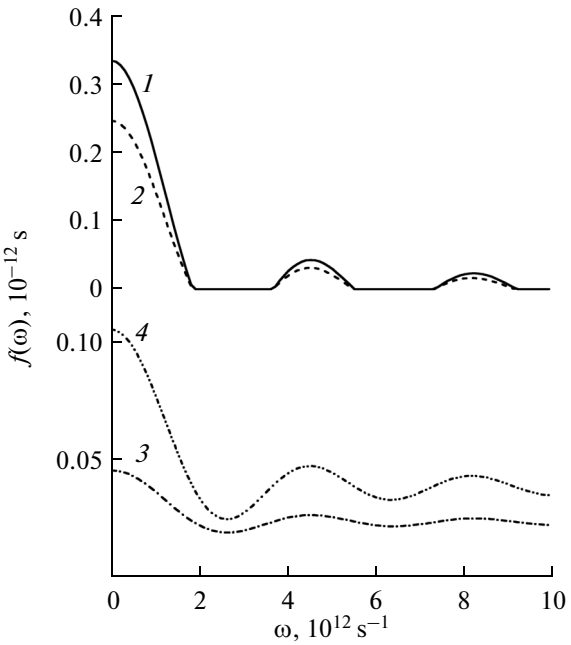

Fig. 2. Phonon spectra of a lead film on graphene as obtained by bombardment of the target with Xe_{13} clusters having an energy of $E_{Xe} = 20$ eV: (*1, 3*) after the first series and (*2, 4*) after the fifth series of impacts. The phonon propagation direction is (*1, 2*) in the plane of the film or (*3, 4*) perpendicular to the film plane.

with the results of quantum-mechanical calculation (−6.98 eV) [17]. The melting point of the Pb_{201} cluster (T_m = 412 K) as we determined from the potential energy jump is consistent with the result of MD calculations (T_m = 417 K) [18] that likewise used the Sutton–Chen potential.

RESULTS AND DISCUSSION

The vertical bombardment of the lead film on graphene with Xe_{13} clusters showed a strong dependence of the outcome of this procedure on the cluster beam energy. Bombardment with a beam energy of 5 eV did not lead to the separation of lead from graphene. Only a few Pb atoms were knocked out of the film, and four lead atoms stuck in divacancies. An increase in the beam energy to 10 eV resulted in the separation of lead from the substrate (Fig. 1). Only several Pb atoms were ablated in this case, whereas the remaining atoms eventually formed above the graphene a cluster offset to the left by approximately twice the length of the graphene sheet along the *ox* axis. The bombardment of the film with a 15-eV beam also resulted in the complete removal of the metal from the graphene, but most of the metal after the end of this procedure appeared in the form of a dense cluster under the graphene, being displaced to the left along the *oy* axis to a distance of about half the width of the graphene sheet. By the impacts of Xe_{13} clusters with an energy of 20 eV, Pb atoms began to hop over the divacancies present in the graphene. As a result, a lead cluster formed under the graphene sheet after the bombardment and only single Pb atoms remained in divacancies or outside of the graphene and the metal cluster. Note that the cluster mechanism of lead separation from graphene clearly dominates in each of the above cases. Impacts of 30-eV clusters caused plastic deformation in the film. The cluster impact-induced slipping of Pb atoms along the graphene surface gave them an opportunity to find the cells produced by C atoms and get stuck in them. This led to an increase in the distance between the carbon atoms and, consequently, a decrease in the size of divacancies. As a result, the Pb atoms could not pass through these defects; they were firmly bound to the divacancy location sites and the other C atoms. In this case, the graphene was not cleared of the metal after the bombardment.

During the bombardment, the dynamics of Pb atoms, especially, the intensity of vertical vibrations significantly altered. Figure 2 shows phonon spectra of the atoms separately for vibrations in the horizontal $f_{xy}(\omega)$ and vertical $f_z(\omega)$ directions after the first and fifth series of bombardment at an energy of 20 eV. In general, these spectra have the same pattern for all energies (starting from 5 eV) of the given range. As can be seen from the figure, both horizontal and vertical vibrations have three characteristic modes, of which the diffusion mode is the most intense. On passing from the first to the fifth series of bombardment runs, the intensity of all peaks in the spectrum of horizontal vibrations are reduced and those in the spectrum of vertical oscillations, on the contrary, significantly increase.

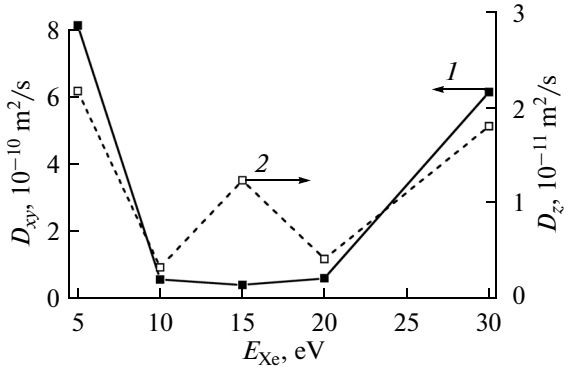

Fig. 3. Components D_{xy} and D_z of the self-diffusion coefficient of Pb atoms in the film, resulting from bombardment of the target with Xe_{13} cluster of different energies E_{Xe}.

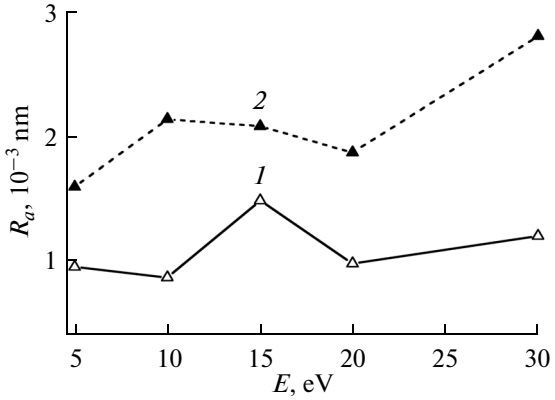

Fig. 5. Graphene roughness produced by target bombardment with (*1*) Xe_{13} and (*2*) Ar_{13} clusters of different energies E.

The mobility of Pb atoms in the horizontal direction, D_{xy}, is usually at least an order of magnitude greater than that in the vertical direction, D_z (Fig. 3). As the cluster beam energy increases from 5 to 10 eV, D_{xy} sharply decreases, a change that is due to the formation of a dense lead cluster separating from the graphene during the bombardment. At beam energies of 15 and 20 eV, the low values of D_{xy} achieved as a result of total bombardment are conserved. In the former case, the reason for this was the same as at a beam energy of 10 eV; in the latter case, vertical displacements of Pb atoms during the bombardment dominate over the horizontal ones. However, at a beam energy of 30 eV, the mobility D_{xy} of lead atoms is greatly increased. In this case, as at a beam energy of 5 eV, the metal is not separated in a significant amount from the graphene. The slippage of Pb atoms associated with plastic deformation of the film is the main cause of the growth in D_{xy}. The behavior of D_z is very similar to that of $D_{xy}(E_{Xe})$. The main difference is a marked increase in D_z at an energy of $E_{Xe} = 15$ eV. This is due to the presence of a certain number of Pb atoms that accompany the removal of the lead cluster from the graphene sheet and are not attached to the cluster. The greatest total self-diffusion coefficient ($D = D_{xy} + D_z$) in the Pb film corresponds to cluster bombardments at an energy of 5 eV ($D = 10.3 \times 10^{-10}$ m^2/s). This value is still below the value of $D = (11.4–23.6) \times 10^{-10}$ m^2/s obtained by MD calculation for liquid lead [19].

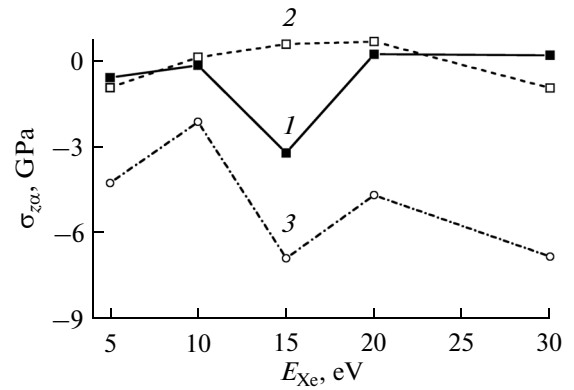

Fig. 4. Stress components (*1*) σ_{zx}, (*2*) σ_{zy}, and (*3*) σ_{zz} in the Pb film plane, resulting from bombardment of the target with Xe_{13} cluster of different energies E_{Xe}.

All the three (σ_{zx}, σ_{zy}, and σ_{zz}) principal stress components in the Pb film (cluster) are of the same order of magnitude (Fig. 4). Energy dependence curves $\sigma_{zx}(E_{Xe})$ and $\sigma_{zz}(E_{Xe})$ exhibit dips at $E_{Xe} = 15$ eV, which are due the fact that the lead cluster in this case was produced not only from the portion of the film separated from graphene, but also from single Pb atoms knocked out of the film and attached to this entity. The low value of components σ_{zz} at $E_{Xe} = 30$ eV is due to the plastic "flow" of the film material.

The bombardment of the Pb film with Xe_{13} clusters affects the state of the graphene surface, which is assessed as surface roughness R_a. Because of the presence of the Pb film screening the impacts of the clusters, the change in $R_a(E_{Xe})$ is not a monotonic function (Fig. 5). The minimum and maximum values of R_a are observed at 10 and 15 eV, respectively. When knocked-off metal atoms move upward, as is the case of $E_{Xe} =$ 10 eV, they shield in the best way the graphene from cluster strikes. When the Pb atoms moved from the graphene preferentially rush in the opposite direction, i.e., downward, as in the case of $E_{Xe} = 15$ eV, they cannot protect graphene from impacts. If the film is pushed into the plastic state, it also poorly resists bombardment and the graphene acquires quite a high values of R_a as a result. Figure 5 also presents data on the roughness, which appears in graphene after vertical Ar_{13} bombardments of graphene-coating copper films [20]. An any cluster beam energy in the range examined, the roughness of graphene coated initially by equivalent copper films (using the same film deposi-

tion method and the same number of atoms in the film) is much higher than in the case of lead coating. The excess of R_a for graphene coated with the copper film over that for the lead coating can be as high as by a factor of 2.5 (at $E = 10$ eV). This result can be due to the use of different "projectiles" (Ar for Cu or Xe for Pb), the presence of H atoms and divacancies in the graphene coated with the Pb film, and different mechanisms (individual for Cu and a cooperative for Pb) of separation of metal films from graphene. The main difference between the bombardments with Ar and Xe beams is associated with a higher (by a factor of 1.81) velocity of Ar atoms in the beam of the same energy, since the velocity ratio is $v_{Ar}/v_{Xe} = \sqrt{m_{Xe}/m_{Ar}}$.

Graphene, covered initially with a lead film, withstood the test of bombardment with heavy inert gas atoms having energies up to 30 eV. Xenon-cluster beam radiation preserved hydrogen on graphene and did not result in the destruction of its edges. The bombardment of nonhydrogenated, copper film-coated graphene with Ar atoms having the same energy resulted in a significant damage to the edges of the graphene sheet [21].

CONCLUSIONS

The removal of deposited lead from graphene surface by bombardment with Xe_{13} clusters having an energy of 5–30 eV and an incidence angle of 0° has been studied using computer simulation. Complete graphene cleaning is not achieved unless the cluster beam energies are as high as 10 and 15 eV. In either case, the debonded lead collects into clusters. But the horizontally displaced lead cluster appears over the graphene sheet in the former case and under the sheet in the latter case. At higher energies of incident clusters, a possible outcome of bombardment can be film "climbing" onto the back side of graphene through divacancies, the "foliation" of the film, and its sticking to the front side of the graphene sheet. The dynamics of Pb atoms significantly alters during the cluster bombardment run. The phonon diffusion peak shows a reduction in the intensity that characterizes the movement of atoms in the horizontal directions and a significantly growth in the intensity corresponding to the vertical vibrations. In the cases of separation of the Pb cluster from the graphene surface, a decrease in both horizontal and vertical mobility of the metal atoms is observed. The drop in vertical mobility can be partially compensated for by the addition of some metal atoms, knocked out of the graphene-supported film, to the Pb cluster already removed from the graphene. Such addition has an effect on the values of some components of the stress tensor; in particular, a decrease in σ_{zy} and σ_{zz} standing out of the general pattern is observed. The removal of the separated Pb cluster upwardly from the graphene sheet reduces its surface roughness, i.e., protects graphene from cluster impacts, and the downward displacement of the cluster significantly increases the roughness of the graphene surface.

ACKNOWLEDGMENTS

This work was supported by the Russian Foundation for Basic Research, project no. 13-08-00273.

REFERENCES

1. Ding, Z., Hu, X., Morales, V.L., and Gao, B., *Chem. Eng. J.*, 2014, vol. 257, no. 12, p. 248.
2. Galashev, A.E. and Rakhmanova, O.R., *Usp. Fiz. Nauk*, 2014, vol. 184, no. 10, p. 1045.
3. Gillen, G. and Roberson, S., *Rapid Commun. Mass Spectrom.*, 1998, vol. 12, no. 19, p. 1303.
4. Gao, H., Zhou, J., Lu, M., Fa, W., and Chen, Y., *J. Appl. Phys.*, 2010, vol. 107, no. 11, p. 114311.
5. Ma, D. and Yang, Z., *New J. Phys.*, 2011, vol. 13, no. 12, p. 123018.
6. Tersoff, J., *Phys. Rev. Lett.*, 1988, vol. 61, no. 25, p. 2879.
7. Stuart, S.J., Tutein, A.V., and Harrison, J.A., *J. Chem. Phys.*, 2000, vol. 112, no. 14, p. 6472.
8. Rafii-Tabar, H., *Phys. Rep.*, 2000, vol. 325, no. 6, p. 239.
9. Kim, Y.M. and Kim, S.C., *J. Korean Phys. Soc.*, 2002, vol. 40, no. 2, p. 293.
10. Arkundato, A., Su'ud, Z., Abdullah, M., and Sutrisno, W., *Int. J. Appl. Phys. Mat.*, 2013, vol. 3, no. 1, p. 1.
11. Li, F.Y. and Berry, R.S., *J. Phys. Chem.*, 1995, vol. 99, no. 9, p. 2459.
12. Ziegler, J.F., Biersack, J.P., and Littmark, U., *The Stopping and Ranges of Ions in Matter*, vol. 1: *The Stopping and Ranges of Ions in Solids*, New York: Pergamon, 1985.
13. Delcorte, A. and Garrison, B.J., *J. Phys. Chem. B*, 2000, vol. 104, no. 29, p. 6785.
14. Lamari, F.D. and Levesque, D., *Carbon*, 2011, vol. 49, no. 15, p. 5196.
15. Berendsen, H.J.C., Postma, J.P.M., van Gunsteren, W.F., DiNola, A., and Haak, J.R., *J. Chem. Phys.*, 1984, vol. 81, no. 8, p. 3684.
16. Galashev, A.E. and Galasheva, A.A., *High Energy Chem.*, 2014, vol. 48, no. 2, p. 112.
17. Davydov, S.Yu., *Phys. Solid State,* 2012, vol. 54, no. 4, p. 875.
18. Jin, Z.H., Sheng, H.W., and Lu, K., *Phys. Rev. B*, 1999, vol. 60, no. 1, p. 141.
19. Belashchenko, D.K., *Usp. Fiz. Nauk*, 2013, vol. 183, no. 12, p. 1281.
20. Galashev, A.E. and Polukhin, V.A., *J. Surf. Invest. X-ray, Synchrotron Neutron Technol.*, 2014, vol. 8, no. 5, p. 1082.
21. Galashev, A.E. and Polukhin, V.A., *Phys. Met. Metallogr.*, 2014, vol. 115, no. 7, p. 697.

Translated by S. Zatonsky